

Nanocomposite cotton gauze cloth with *in situ* generated silver, copper and their binary metal nanoparticles by bioreduction method

Basa Ashok^a, M.P. Indira Devi^b, P. Sivaranjana^c,

AnumakondaVarada Rajulu^d, Sikiru Oluwarotimi Ismail^e,

Faruq Mohammad^f, Hamad A. Al-Lohedan^f, Rajini Nagarajan^{g,*}

^a Department of Physics, University College of Engineering, Osmania University,
Hyderabad 500007, India.

^c Department of Chemistry, Kalasalingam Academy of Research and Education, Krishnankoil,
Tamil Nadu, 626126, India.

^{b,d,g*} Centre for Composite Materials, Department of Mechanical Engineering, Kalasalingam
Academy of Research and Education, Krishnankoil, Tamil Nadu, 626126, India.

^e Department of Engineering, School of Physics, Engineering and Computer Science,
University of Hertfordshire, Hatfield, AL10 9AB, Hertfordshire, England, United Kingdom

^f Department of Chemistry, College of Science, King Saud University, P.O.Box 2455, Riyadh,
Kingdom of Saudi Arabia 11451

Corresponding author: Rajini Nagarajan, E-mail: rajiniklu@gmail.com; Telephone: +91 99421 39392; Fax: +91 4563 289042.

Abstract

In the present work, the authors prepared nanocomposite cotton gauze cloth (NCGC) by *in situ* generating the nanoparticles of silver (ANPs) and copper (CuNPs) and their binary metallic nanoparticles (BMNPs) using aqueous extraction of *Azadirachta indica* leaves as a reducing agent. The NCGCs had roughly spherical AgNPs, CuNPs and BMNPs in the size range of 50 to 120nm. The corresponding mean size of the spherical AgNPs, CuNPs and BMNPs was 94nm, 89nm and 87nm respectively. The participation of the hydroxyl and amino groups of the leaf extract in the generation of the metal nanoparticles in the NCGCs was established by studying the chemical interactions. All the NCGC specimens exhibited significant antibacterial activity. However, the NCGCs with BMNPs had higher antibacterial efficiency when compared to those with homo metal nanoparticles. Hence, the NCGC with generated BMNPs can be effectively used as antibacterial wound dressing material.

Keywords: Nanocomposite, cotton gauze cloth, *in situ* generation, synergetic effect, antibacterial activity.

1. Introduction

Global perspective on the development of conducive eco-friendly sustainable environment encompassed the researchers to explore the applicability in various domains. Nowadays, medical outlets need effective waste management system to minimize the greenhouse effect. Cotton fabric is one of the textile products in the field of medical industry extensively used for wound healing and secondary level usage. Further, the modified cotton fabric with the medical benefits is the immediate need for the society to the larger extent. In general, the Meditech (medical textile) products can be classified into four categories, which include health care and hygiene products, non-implantable medical textile, implantable medical textile and extra corporeal. The cotton gauze can immobilize the enzymes by forming covalent bond with free amino groups. Thus, cotton gauze bandage is a promising biocatalytic supporting the biomedical field.^[1] All the above mentioned categories of products were mainly used in surgical and hospital wards to prevent spread of infections.^[2] If these products could be made available with antimicrobial property to prevent against infections then it becomes more appropriate for the biomedical applications. The antimicrobial property of metal nanoparticles was extensively studied and reported by many researchers. The incorporation of nanometal particles into the fabric as filler will impart antimicrobial property and in addition it will also add up water repellent property, wrinkle

resistance, shrink proof, UV resistance, controlled hydrophilicity/ hydrophobicity to the fabric. The bioreduction of metal salts to the nano state using plant extracts and agro waste materials was found to be simple, economic as well as eco-friendly approach. Recently, many works on bioreduction of metal salts to their respective nanoparticles have been reported in the literature. Aravinthan et al.^[3] synthesized AgNPs using aqueous extract of sunroot tuber as a bioreductant. The synthesized AgNPs were in the size range of 10-70 nm and showed good antibacterial activity. Govarathanan et al.^[4] used panchakavya to synthesize the AgNPs which exhibited good antibacterial activity. Lee et al.^[5] synthesized AgNPs using cow milk and reported good antifungal activity against pathogens. Muthusamy et al.^[6] generated AgNPs using *Spirulina* microalgae which exhibited excellent antibacterial activity. Govarathanan et al.^[7] also synthesized AgNPs using low cost coconut oil cake extract and studied their antibacterial activity. In another study, Govarathanan et al.^[8] used cottonseed oil cake extract as a bioreductant to synthesize AgNPs and studied their antibacterial and cytotoxicity activity. Valarmathi et al.^[9] generated AgNPs using marine seaweed *Spyridia filamentosa* and studied their clinical applications. Ameen et al.^[10] synthesized AgNPs by mediating soil bacterial *Cupriavidus sp.* and the synthesized nanoparticles exhibited excellent antibacterial activity. Ameen et al.^[11] also generated AgNPs using *Mangifera Indica* flower extract and the generated nanoparticles showed good antibacterial activity. Mythili et al.^[12] synthesized AgNPs utilizing market vegetable waste which exhibited good antibacterial activity.

Almost all parts of the plants such as their leaves, fruits, flowers, stem, bark, fruit peel and root were employed as bioreductant.^[13-16] The existence of flavanoids, alkaloids, phenols and polyphenols in the plants are responsible for reducing the metal salts to their nano state. The flavonoids are the polyhydroxylated secondary metabolite in plants with –OH groups which reduce the metal salt solutions to the nano state.^[17] The flavonoids^[15] were reported to be the major contributors of reducing the metal while the other compounds play their role as capping agents thereby descending the agglomeration of nanometal particles. The process of addition of nanometal particles as fillers into the polymer matrices was reported.^[18] The real barrier lies in achieving the uniform dispersion of the nanometal particles into polymer matrix. The high surface energy of the nanometal particles incline to get agglomerated even before dispersing them into the polymer matrix. Few researchers have adopted the method of *in situ* generation^[19] of nanometal particles inside the polymer matrix. The polymer molecules stabilise the nanometal particles there by preventing agglomeration. The copper

(CuNPs)^[16] and silver (AgNPs)^[17] nanoparticles were generated in cellulose employing plant extracts thereby forming the nanocomposites. These composite films possessed appreciable tensile strength of up to 152 MPa, thermal stability up to 300 °C and antibacterial activity against *E-coli* bacteria which makes them suitable to be used as packing materials.

The CuNPs ^[20] and AgNPs ^[21] were generated inside the cotton fabrics using *Cassia alata* ^[22], Red sanders powder ^[23], aloe vera ^[24], *Moringaoliefiera* ^[25], *Senna auriculata* ^[26], *Pongamia pinnata* ^[27], *Ocimum sanctum* ^[15], *Vitex negundo* ^[28] and date seed extract. ^[29] In all the above cases, the developed nanocomposite cotton fabrics possessed antibacterial activity against a wide range of bacterial strains. The antibacterial activity was retained for repeated usage. The CuNPs were found to be more effective against *B. subtilis* species, CuONPs were effective against *S aureus*, meticillin-resistant *S. aureus*, *S.epidermidis*, *E. coli*, and *P. aeruginosa* whereas AgNPs were found to be effective against *E. coli* and *S. aureus*. The CuNPs ^[30] get adhered to the bacterial cell wall due to opposite electrical charges and reduces the cell wall. The cavities and pits were formed in the cell wall which result in the change in the shape of the cell from rod form to formless. The cavity and pit formation in the cell wall leads to leakage of the fluid thereby denaturation of protein takes place and result in killing the cell. The AgNPs ^[31] interact with bacterial cells resulting in the interaction with lipids and proteins, free radical generation and damage to DNA. The CuNPs and AgNPs were found to be effective against a wide range of bacterial strains.

Besides, the researchers also adopted a new strategy of developing bimetallic nanoparticles inside the cotton fabric using aloe vera ^[24] leaf extract and red sanders powder ^[32] as bioreductants. The ultimate aim of developing bimetallic nanoparticles is to have the advantage of both CuNPs and AgNPs in the same system. The bimetallic nanoparticles were more advantageous over the homo metallic nanoparticle system. The bimetallic nano particles exhibit superior antimicrobial response against bacterial strains as the generated metal nanoparticles were more in number and the average size of the generated nanoparticles decreased.

After analysing all the above said aspects, there was a scope to explore the bimetallic systems with different environments. Therefore, the new combinations of sources can influence the structure-property of the fabricated material. Accordingly, this present work addresses the fabrication of nanocomposite cotton gauge cloth (NCGC) with *in situ* generated copper, silver and their binary nanoparticles by using *Azadirachta indica* leaf extract as

reducing agent by bioreduction method. The NCGC specimens were characterized by electron microscopy, X-ray, spectral and antibacterial tests.

2. Experimental

2.1 Materials used

White cotton gauge cloth (CGC) procured from the local pharmaceutical shop was used after cleaning and drying. Mature leaves of *Azadirachta indica* tree in the local garden were used after cleaning and wiping out with clean cloth. AgNO₃ (Sigma Aldrich) and CuSO₄.5H₂O (S.D. Chemicals, India) were used as received. In all the works, deionized water was used.

2.2 Methods and Testing

2.2.1 Preparation of *Azadirachta indica* leaf extract

For the preparation of 10 wt.% leaf extract, 100g of cleaned *Azadirachta indica* leaves were added to 900g of hot water (80 °C) and maintained at that temperature for a period of 20 minutes. After cooling, the decoction with 10 wt.% leaf extract was filtered and kept in a refrigerator (5 °C) until it was utilized.

2.2.2 Making the matrix

The leaf extract prepared was taken in a glass container and the gauze cloth specimens (30 cm X 6 cm) were immersed by rolling and the container was kept on a magnetic stirrer at ambient conditions and moderate speed of 300 rpm for 24 hours. During this period, CGC turned light brown and remained unchanged even when washed indicating infusion of the leaf extract. These cleaned matrix materials were air dried and stored in desiccators till used.

2.2.3 Preparation of the NCGC specimens

In order to generate the homo metal particles (NPs), the corresponding aqueous metal solutions of 5 mM concentration were prepared. For generating binary metal NPs (BMNPs), equimolar (2.5mM) solutions of both metal salt solutions were prepared and mixed together. In each solution, the matrix specimens were immersed and stirred at 300rpm on magnetic stirrer for 24 hours at ambient conditions. The NCGCs with generated metal NPs showed a color change which remained unchanged even after repeated washings. This indicates the permanent generation of NPs in the NCGCs. The cleaned NCGCs were dried in the air and sealed in polyethylene covers.

2.2.4 Scanning Electron Microscopy

For visualizing the homo NPs and BMNPs in the NCGCs, the SEM analysis was carried (Zeiss EVO 18 scanning electron microscope). An operating voltage of 10 kV was maintained during the recording of the micrographs of the gold coated specimens. For elemental analysis, the EDX spectral analysis was carried using the same microscope.

2.2.5 Infrared spectral analysis

To probe the possible interactions between the matrix and the generated NPs in the NCGCs, the FTIR spectra were recorded (Smart iTR ATR Nicolet is10 spectrophotometer) in the 4000-500 cm^{-1} range. In each case the conditions of 32 scans and resolution of 4 cm^{-1} were maintained.

2.2.6 X-ray diffraction

X-ray diffractograms of the CGC, matrix and NCBCs were recorded using Bruker D8 Discover diffractometer in $2\theta=10^\circ$ to 80° range at a scanning rate of $2^\circ/\text{min}$ with the operating conditions of 40 kV and 25 mA.

2.2.7 Antimicrobial analysis

The antibacterial test of NCGCs and matrix was carried using disc method. [33] The disc method was carried out against both Gram^{-ve} and Gram^{+ve} bacteria. The formed clear zones which are indicative of bacterial inhibition were photographed. The diameters of clear zones were measured using Image J software.

3. Results & discussion

3.1 Physical observation of NCGCs

To notice the changes taking place in gauge cloth, matrix and the NCGCs with generated AgNPs, CuNPs and BMNPs, the images are presented in Fig.1.

Fig. 1 Photographs of (a) gauge cloth; (b) matrix and NCGCs with (c) AgNPs; (d) CuNPs and (e) BMNPs.

From Fig.1 it can be deduced that matrix (Fig.1b) appeared light brown compared to the white color of the gauge cloth (Fig.1a). On the other hand, the NCGCs having AgNPs changed to medium brown (Fig. 1c) while the NCBC with CuNPs was with gray color.

Further, the NCBC with BMNPs appeared dark brown (Fig. 1e). The change in color of the NCGCs when compared to the matrix indicates the generation of corresponding NPs. For further confirmation, the microscopic investigation was made.

3.2 Scanning Electron Microscopy

To visualize the generated AgNPs, CuNPs and their BMNPs in the bandage cloth the, micrographs of NCGCs with generated AgNPs, CuNPs and BMNPs are shown in Fig.2a, 2b and 2c respectively. The respective EDX spectra are depicted in Fig.2d, 2e and 2. The histograms representing the particle distribution of the NCGCs having the generated AgNPs, CuNPs and BMNPs are respectively presented in Fig. 2g, 2h and 2i.

Fig. 2 SEM images of NCGCs having (a) AgNPs, (b) CuNPs and (c) BMNPs; EDX spectra of NCGCs with (d) AgNPs, (e) CuNPs and (f) BMNPs; Histograms of NCGCs with (g) AgNPs, (h) CuNPs and (i) BMNPs

From Fig.2 (a, b and c), it can be seen that the generated AgNPs, CuNPs and BMNPs are roughly spherical in shape. Further, Fig.2 (a, b and c) indicates that few CuNPs were generated, medium number of AgNPs were generated while more number of BMNPs were generated in the NCGCs. The synergy may be responsible for the presence of large number of BMNPs. The EDX spectra Ag (Fig.2d), Cu (Fig.2e) and (Ag+Cu) (Fig.2f) indicate the presence of respective metal element in the NCGCs. From the histograms of the NCGCs with AgNPs (Fig.2g), CuNPs (Fig.2h) and BMNPs (Fig.2i), it is evident that in all the cases, the generated NPs were in the range of 50nm – 120 nm. The mean sizes of the AgNPs, CuNPs and the BMNPs were found to be 94 nm, 89 nm and 87 nm respectively. These observations indicate that the average size of the BMNPs in NCBCs is lower than those with homo metallic NPs. Similar observation was made by Mamata et al.^[24] in the case of NCBCs with BMNPs using aloe vera leaf extract as a reducing agent. These observations suggest that more number of BMNPs were generated in the NCGCs due to the synergetic effect.

3.3 FTIR Spectroscopy Analysis

The FTIR spectral analysis was carried out to know the molecular interactions of the generated NPs with the matrix in the NCGCs. The FTIR spectra of bandage cloth, matrix and NCBCs with *in situ* generated AgNPs, CuNPs and BMNPs are depicted in Fig. 3. Fig.3 indicates that the spectra have similar peaks with slight variation in intensity. For instance, both the matrix and bandage cloth contain similar molecular functionalities. The peaks at

3315 cm^{-1} , 2877 cm^{-1} , 1631 cm^{-1} , 1429 cm^{-1} , 1331 cm^{-1} , 1001 cm^{-1} and 668 cm^{-1} indicate –OH alcohol stretching, aldehyde –CH st, C-C st, C-O and C-H b, symmetric C-H st, C-O st hydroxyl groups of flavonoids present in neem extract and out of plane bending vibrations of OH and CH groups, respectively.^[34-38] The matrix exhibited an additional peak at 2354 cm^{-1} , corresponding to OH acidic functional group of amino acids present in proteins of neem extract. From Fig.3, it can also be seen that the matrix exhibited higher peak intensities at 3315 cm^{-1} and 2877 cm^{-1} due to diffusion of hydroxy and aldehyde functional groups of leaf extract into the bandage cloth during the preparation of the matrix. There is no change in peak intensity for the other peaks. FTIR spectra of NCGCs indicate that the peaks of NCGCs with AgNPs, CuNPs and BMNPs exhibited similar peaks with variation of intensity for some peaks. The peak at 3317 cm^{-1} of NCGCs exhibited lower intensity than the matrix. This reveals that the hydroxyl groups present in the matrix took part in the generation of the NPs in the NCGCs.

Fig. 3 Spectra (FTIR) of cotton gauge cloth, matrix and NCGCs

The other peak at 2891 cm^{-1} was related to aldehydic CH stretching functional group. The NCBC with BMNPs exhibited higher intensity of peak at 2347 cm^{-1} (OH acidic) than that of matrix and NCGCs with AgNPs and CuNPs. It may be due to catalytic oxidation of CHO functional groups in the matrix by the generated AgNPs and CuNPs on the gauge cloth. However, the NCGCs exhibited similar peaks and same intensity with that of matrix at 1987 cm^{-1} , 1636 cm^{-1} , 1441 cm^{-1} , 1309 cm^{-1} , 1001 cm^{-1} and 679 cm^{-1} . The FTIR spectra confirm the formation of the AgNPs, CuNPs and BMNPs on the cotton gauge cloth by bio reduction with hydroxyl functional groups.

3.4 X-ray analysis

In order to further confirm the *in situ* generation of the MNPs in the NCBCs, the X-ray analysis was carried. The diffractograms of the CGC, matrix and the NCBCs are presented in Fig. 4(a).

Fig.4 X-ray diffractograms of (a) cotton gauge cloth, matrix and NCBCs; (b) NCBC with in situ generated AgNPs; (c) NCBC with in situ generated CuNPs and (d) NCBC with in situ generated BMNPs.

From Fig.4 (a), it is evident that there are mainly two intense common peaks in all the samples. The two peaks at $2\theta=15.5^\circ$ and 23° arose due to the reflections from the (101) and (002) planes respectively of cellulose-I structure^[32]. The other common peak at around $2\theta=34^\circ$ may be due to the impurities in the bandage cloth. From Fig.4 (a), the peaks of the MNPs in NCBCs are not clear as the high intensity cellulose-I peaks obscured them. In order to visualize them, the diffractograms of NCBCs with *in situ* generated AgNPs, CuNPs and BMNPs are expanded in the $2\theta=30^\circ-80^\circ$ range and presented in Fig.4 (b), 4(c) and 4(d) respectively. The peak positions are indicated in the respective diffractograms. From Fig.4 (b), of the many peaks observed, those at $2\theta=38.2^\circ$, 45.4° , 64.2° and 77.3° arose due to the reflections of (111), (200), (220) and (311) planes respectively of AgNPs^[32]. In Fig.4(c), the peak at $2\theta=43.4^\circ$ was due to the (111) plane of CuNPs. The other peak at $2\theta=39.5^\circ$ arose due to the reflections from the (111) plane of CuO^[24]. This indicates that some of the CuNPs generated might have been oxidized to CuO NPs as copper is a good oxidizing agent^[24]. The other peaks observed in Fig.4 (b) and 4(c) may be due to the chemical groups of the leaf extract used as the reducing agent. In Fig.4 (d) (NCBCs with BMNPs), the peaks corresponding to both AgNPs and CuNPs are observed. These observations further confirm the *in situ* generation of MNPs in the NCBCs.

3.5 Mechanism of generation of the NPs in NCGCs

Azadirachta indica (AI) Lynn plant leaves contain hydroxyl functional groups in the form of flavonoids. Quercetin is one of the major constituents among the different flavonoids present in AI leaves.^{[38][39]} The FTIR analysis revealed that the hydroxyl functional groups are involved in the bioreduction of Ag^+ , Cu^{+2} ions and bimetallic (Ag^+ and Cu^+) ions into AgNPs, CuNPs and their BMNPs. A schematic feasible mechanism was proposed which is presented in Scheme 1 and it is evident that the two -OH groups in Quercetin were involved in the bioreduction of 2Ag^+ and 2Cu^{+2} ions into metallic silver and copper and their BMNPs. The utilization of two hydroxyl functionalities for the reduction of 2Ag^+ and 2Cu^{+2} ions was also reported by earlier researchers.^{[40][41]} The reduced silver and copper ions form a complex with Quercetin and on rearrangement forms individual AgNPs, CuNPs and their BMNPs.

Scheme 1. Mechanism of generation of AgNPs, CuNPs and BMNPs in the NCGCs by the *Azadirachta indica* leaf extract.

The mechanism presented above indicates the generation of the NPs by electrostatic interactions between OH and metal ions in the NCGCs.

3.6 Antibacterial activity

To examine the antibacterial activity of NCGCs under study, the disc method was carried against two Gram^{-ve} (*E.coli*, *P.aeruginosa*) and two Gram^{+ve} (*B.licheniformis*, *S.aureus*) bacteria. The images of the inhibition zones formed by the matrix (if any) and the NCGCs are shown in Fig.5. The labelling of the samples is indicated in the parenthesis as – matrix (a), NCBC with generated AgNPs (b), CuNPs (c) and BMNPs (d).

Fig. 5 Images of the inhibition zones formed by Matrix (a) and NCGCs with generated ANPs (b), CuNPs (c) and BMNPs (d) against Gram^{-ve} (*E.coli*, *P.aeruginosa*) and Gram^{+ve} (*B.licheniformis*, *S.aureus*) bacteria.

From Fig.5, it is clear that the matrix did not form any inhibition zone indicating its inability to inhibit the growth of the bacteria. On the other hand, the NCGCs formed significant inhibition zones against all the tested bacteria. The measured clear zone diameters in each case are given in Table 1.

Table 1. Inhibition zone diameters of the matrix and the NCGCs against Gram^{-ve} (*E.coli* and *P.aeruginosa*) and Gram^{+ve} (*B. licheniformis* and *S.aureus*) bacteria.

Table 1 indicates that the inhibition zone diameters varied for NCGCs with AgNPs in the range of 11.5 mm to 14.5 mm and with CuNPs in the range of 12.9 mm to 15.0 mm. On the other hand, the NCGCs with BMNPs formed inhibition zones in the range of 17.8 mm to 20.1 mm. These observations clearly indicate that the NCGCs with BMNPs exhibited higher inhibition efficiency against the bacteria when compared to the NCGCs with homo metal nanoparticles. This may be due to the synergy of both the metals in the NCGC with BMNPs. Mamatha et al. [24] reported a similar observation for cotton fabrics with generated BMNPs employing aloe vera extract as a bioreductant. Hence NCBC with BMNPs can be utilized more effectively as antibacterial dressing material in the medical field.

Conclusions

Sustainable eco-friendly NCGC specimens with *in situ* generated AgNPs, CuNPs and BMNPs were fabricated using simple cost-effective method for small scale biomedical applications. In this work, aqueous extract of *Azadirachta indica* leaves was successfully used to reduce the metal salts to their respective NPs. The change in the colour between the matrix and NCBCs from the macroscopic visual inspection indicated the formation of

different metal nanoparticles in the matrix. The microscopic investigation indicated the *in situ* generation of the NPs in NCBCs with sizes in the range of 50 nm – 120 nm. Further, the mean sizes of the AgNPs, CuNPs and the BMNPs generated in the NCGCs were found to be 94 nm, 89 nm and 87 nm respectively. The presence of hydroxyl and amino groups (observed from the FTIR analysis) were identified to be responsible for the generation of NPs in the NCGCs. The X-ray analysis also indicated the generation of the respective metal NPs in NCBCs. Maximum antibacterial properties were noticed for the NCGCs with BMNPs irrespective of the bacteria when compared to the other systems. The synergistic effect of AgNPs and the CuNPs in the NCGCs with BMNPs was found to be responsible for the higher efficiency of antibacterial activity. Eventually, these NCGCs with BMNPs can be recommended as antibacterial wound cleaning and dressing materials.

Acknowledgment

We hereby acknowledge and sincerely appreciate unalloyed supports from the managements of the following institutions: Osmania University, Hyderabad, India as well as the Kalasalingam Academy of Research and Education, Tamil Nadu, India. The King Saud University authors acknowledge the funding from Researchers Supporting Project (RSP-2021/355), King Saud University, Riyath, Saudi Arabia.

References

1. Seabra, I. J.; Gil, M. H. Cotton Gauze Bandage: A Support for Protease Immobilization for Use in Biomedical Applications. *Rev. Bras. Ciencias Farm. J. Pharm. Sci.*, **2007**, 43 (4), 535–542. DOI: 10.1590/S1516-93322007000400006.
2. Simões, D.; Miguel, S. P.; Ribeiro, M. P.; Coutinho, P.; Mendonça, A. G.; Correia, I. J. Recent Advances on Antimicrobial Wound Dressing: A Review. *European Journal of Pharmaceutics and Biopharmaceutics*. Elsevier B.V. June 2018, pp 130–141. DOI:10.1016/j.ejpb.2018.02.022.
3. Aravinthan, A.; Govarathanan, M.; Selvam, K.; Praburaman, L.; Thangasamy Selvankumar, T.; Balamurugan, R.; Kamala Kannan, S.; Jong, H.K. Sunroot mediated synthesis and characterization of silver nanoparticles and evaluation of its antibacterial and rat splenocyte cytotoxic effects. *Int J Nanomedicine.*, **2015**, 10, 1977-1983. DOI: 10.2147/IJN.S79106. eCollection 2015.
4. Govarathanan, M.; Selvankumar, T.; Manoharan, K.; Rathika, R.; Shanthi, K.; Jae Lee, J.K.; Cho, M.; Kamaala Kannan, S.; Taek Oh, B.T. Biosynthesis and characterization of silver nanoparticles using panchakavya, an Indian traditional farming formulating agent. *Int J Nanomedicine.*, **2014**, 9, 1593-1599. DOI: 10.2147/IJN.S58932. eCollection 2014.
5. Lee, J.K.; Sung, H.P.; Govarathanan, M.; Wang, H.P.; Young, S.S.; Cho, M.; Wang, H.L.; Lee, Y.; Kannan, J.; Seralathan Kamala Kannan, S.; Oh, T.B. Synthesis of silver nanoparticles using cow milk and their antifungal activity against phytopathogens. *Mater. Lett.*, **2013**, 105, 128-131. DOI :10.1016/j.matlet.2013.04.076.
6. Govarathanan, M.; Selvankumar, T.; Mythili, R.; Sudhakar, C.; Selvam, K. Biosynthesis of silver nanoparticles from *Spirulina* microalgae and its antibacterial activity. *Environ. Sci. Pollut. Res.*, **2017**, 24, 19459–19464. DOI 10.1007/s11356-017-9772-0.
7. Govarathanan, M.; Young, S.S.; Lee, J.K.; Jung, I.B.; Ju, H.J.; Kim, J.S.; Min, C.; Kamala Kannan, S.; Oh, B.T. Low-cost and eco-friendly synthesis of silver nanoparticles using coconut (*Cocos nucifera*) oil cake extract and its antibacterial activity. *Artif Cells Nanomed Biotechnol.*, **2016**, 44(8), 1878-1882. DOI:10.3109/21691401.2015.1111230.

8. Govarthan, M.; Min,C.; Park,J.H.; JangJ.S.; Yi,Y.J.; Kamala Kannan, S.; Oh,B.T. Cottonseed Oilcake Extract Mediated Green Synthesis of Silver Nanoparticles and Its Antibacterial and Cytotoxic Activity. *J. Nanomater.*, **2016**. 1-6. DOI:10.1155/2016/7412431.
9. Valarmathi, N.; Ameen, F.; Almansob,A; Kumar,P.; Arunprakash,S.; Govarthan, M. Utilization of marine seaweed *Spyridia filamentosa* for silver nanoparticles synthesis and its clinical applications. *Mater. Lett.*, **2020**. 263, 127244. DOI:10.1016/j.matlet.2019.127244.
10. Ameen, F.; AlYahia, S.; Govarthan, M.; ALjahdali, N.; Al-Enazi, N.; Alsamhari, K.; Alshehri, W.A.; Alwakeel, S.S.; Alharbi, S.A. Soil bacteria *Cupriavidus* sp. mediates the extracellular synthesis of antibacterial silver nanoparticles. *J. Mol. Struct.*, **2020**. 1202, 127233. DOI:10.1016/j.molstruc.2019.127233.
11. Ameen,F.; Srinivasan,P.; Selvankumar,T.; Kamala Kannan,S.; Al Nadhari,S.; Almansob,A.; Dawoud.T.; Govarthan, M. Phytosynthesis of silver nanoparticles using *Mangifera indica* flower extract as bioreductant and their broad-spectrum antibacterial activity. *Bioogaic Chemistry*. **2019**. 88, 102970. DOI:10.1016/j.molstruc.2019.127233.
12. Mythili, R.; Selvankumar, T.; Kamala Kannan, S.; Sudhakar, C.; Ameen,F.; Al-Sabri,A Selvam, K.; Govarthan, M.; Kim, H. Utilization of market vegetable waste for silver nanoparticle synthesis and its antibacterial activity. *Mater. Lett.*, **2018**.225, 101-104. DOI: 10.1016/j.matlet.2018.04.111
13. Shobha, G.; Moses, V.; Ananda, S. Biological Synthesis of Copper Nanoparticles and Its Impact - a Review. *Int. J. Pharm. Sci. Invent. ISSN*, **2014**, 3 (8), 29–30.
14. Sadanand, V.; Rajini, N.; Satyanarayana, B.; Rajulu, A. V. Preparation and Properties of Cellulose/Silver Nanoparticle Composites with in Situ-Generated Silver Nanoparticles Using *Ocimum Sanctum* Leaf Extract. *Int. J. Polym. Anal. Charact.*, **2016**, 21 (5), 408–416. DOI:10.1080/1023666X.2016.1161100.
15. Sadanand, V.; Rajini, N.; Varada Rajulu, A.; Satyanarayana, B. Preparation of Cellulose Composites with in Situ Generated Copper Nanoparticles Using Leaf Extract and Their Properties. *Carbohydr. Polym.*, **2016**, 150, 32–39. DOI:10.1016/j.carbpol.2016.04.121.

16. Ahmed, S.; Ahmad, M.; Swami, B. L.; Ikram, S. A Review on Plants Extract Mediated Synthesis of Silver Nanoparticles for Antimicrobial Applications: A Green Expertise. *Journal of Advanced Research*. Cairo University 2016, pp 17–28.
DOI:10.1016/j.jare.2015.02.007.
17. Sahu, N.; Soni, D.; Chandrashekhar, B.; Satpute, D. B.; Saravanadevi, S.; Sarangi, B. K.; Pandey, R. A. Synthesis of Silver Nanoparticles Using Flavonoids: Hesperidin, Naringin and Diosmin, and Their Antibacterial Effects and Cytotoxicity. *Int. Nano Lett.*, **2016**, 6 (3), 173–181. DOI:10.1007/s40089-016-0184-9.
18. Greßler, S.; Prenner, S.; Kurz, A.; Susanne, R.; Pavlicek, A.; Part, F. Polymer Nanocomposites - Additives, Properties, Applications, Environmental Aspects (NanoTrust-Dossier No. 052 – February 2020). *Inst. Technol. Assess.*, **2020**, 52, 6.
DOI:10.1553/ita-nt-052en.
19. Valencia, L.; Kumar, S.; Nomena, E. M.; Salazar-Alvarez, G.; Mathew, A. P. In-Situ Growth of Metal Oxide Nanoparticles on Cellulose Nanofibrils for Dye Removal and Antimicrobial Applications. *ACS Appl. Nano Mater.*, **2020**, 3 (7), 7172–7181.
DOI:10.1021/acsanm.0c01511.
20. Paramasivan, S.; E.R., N.; Nagarajan, R.; Anumakonda, V. R.; N., H. Characterization of Cotton Fabric Nanocomposites with in Situ Generated Copper Nanoparticles for Antimicrobial Applications. *Prep. Biochem. Biotechnol.*, **2018**, 0 (0), 1–8.
DOI:10.1080/10826068.2018.1466150.
21. Sivaranjana, P.; Nagarajan, E. R.; Rajini, N.; Ayrilmis, N.; Rajulu, A. V.; Siengchin, S. Preparation and Characterization Studies of Modified Cellulosic Textile Fabric Composite with in Situ-Generated AgNPs Coating. *J. Ind. Text.*, **2019**, 1–16.
DOI:10.1177/1528083719855312.
22. Sivaranjana, P.; Nagarajan, E. R.; Rajini, N.; Jawaid, M.; Rajulu, A. V. Cellulose Nanocomposite Films with in Situ Generated Silver Nanoparticles Using Cassia Alata Leaf Extract as a Reducing Agent. *Int. J. Biol. Macromol.*, **2017**, 99, 223–232.
DOI:10.1016/j.ijbiomac.2017.02.070.
23. Amara, V. R.; Basa, A.; Mallavarapu, U. M.; Vatti, C.; Gopireddy, S. V.; Anumakonda, V. Preparation and Properties of Cotton Nanocomposite Fabrics with in Situ Generated Copper Nanoparticles Using Red Sanders Powder Extract as a

- Reducing Agent. *Inorg. Nano-Metal Chem.*, **2019**, *49* (10), 343–348.
DOI:10.1080/24701556.2019.1661437.
24. Mamatha, G.; Varada Rajulu, A.; Madhukar, K. In Situ Generation of Bimetallic Nanoparticles in Cotton Fabric Using Aloe Vera Leaf Extract, as a Reducing Agent. *J. Nat. Fibers*, **2020**, *17* (8), 1121–1129. DOI:10.1080/15440478.2018.1558146.
 25. Anand, K.; Murugan, V.; Mohana Roopan, S.; Surendra, T. V.; Chuturgoon, A. A.; Muniyasamy, S. Degradation Treatment of 4-Nitrophenol by Moringa Oleifera Synthesised GO-CeO₂ Nanoparticles as Catalyst. *J. Inorg. Organomet. Polym. Mater.*, **2018**, *28* (6), 2241–2248. DOI:10.1007/s10904-018-0891-y.
 26. Akepogu, P.; Mallavarapu, U.; Gopireddy, V. S.; Seetha, J.; Mesa, A.; Duddela, V.; Anumakonda, V. R. In Situ Generation of Antibacterial Silver Nanocomposite Cotton Fabrics by Bio Route. *Inorg. Nano-Metal Chem.*, **2020**. DOI:10.1080/24701556.2020.1852572.
 27. Kishanji, M.; Mamatha, G.; Madhuri, D.; Suresh Kumar, D.; Vijaya Charan, G.; Ramesh, S.; Jadhav, V.; Madhukar, K. Preparation and Characterization of Cellulose/in Situ Generated Silver Nanoparticle Composite Films Prepared Using Pongamia Pinnata Leaf Extract as a Reducing and Stabilizing Agent. *Inorg. Nano-Metal Chem.*, **2020**. DOI:10.1080/24701556.2020.1822869.
 28. Mamatha, G.; Sowmya, P.; Madhuri, D.; Mohan Babu, N.; Suresh Kumar, D.; Vijaya Charan, G.; Varaprasad, K.; Madhukar, K. Antimicrobial Cellulose Nanocomposite Films with In Situ Generations of Bimetallic (Ag and Cu) Nanoparticles Using Vitex Negundo Leaves Extract. *J. Inorg. Organomet. Polym. Mater.*, **2020**, 1–14. DOI:10.1007/s10904-020-01819-9.
 29. Ramadan, M. A.; Sharawy, S.; Elbisi, M. K.; Ghosal, K. Eco-Friendly Packaging Composite Fabrics Based on in situ Synthesized Silver Nanoparticles (AgNPs) & Treatment with Chitosan and/or Date Seed Extract. *Nano-Structures and Nano-Objects*, **2020**, *22*, 100425. DOI:10.1016/j.nanoso.2020.100425.
 30. Mahmoodi, S.; Elmi, A.; Hallaj Nezhadi, S. Copper Nanoparticles as Antibacterial Agents. *J. Mol. Pharm. Org. Process Res.*, **2018**, *06* (01), 1–7. DOI:10.4172/2329-9053.1000140.

31. Durán, N.; Durán, M.; de Jesus, M. B.; Seabra, A. B.; Fávaro, W. J.; Nakazato, G. Silver Nanoparticles: A New View on Mechanistic Aspects on Antimicrobial Activity. *Nanomedicine: Nanotechnology, Biology, and Medicine*. Elsevier Inc. April 2016, pp 789–799. DOI:10.1016/j.nano.2015.11.016.
32. Venkateswara Rao, A.; Ashok, B.; Uma Mahesh, M.; Venkata Subbareddy, G.; Chandra Sekhar, V.; Venkata Ramanamurthy, G.; Varada Rajulu, A. Antibacterial Cotton Fabrics with in Situ Generated Silver and Copper Bimetallic Nanoparticles Using Red Sanders Powder Extract as Reducing Agent. *Int. J. Polym. Anal. Charact.*, **2019**, 24 (4), 346–354. DOI:10.1080/1023666X.2019.1598631.
33. Varaprasad, K.; Vimala, K.; Ravindra, S.; Narayana Reddy, N.; Venkata Subba Reddy, G.; Mohana Raju, K. Fabrication of Silver Nanocomposite Films Impregnated with Curcumin for Superior Antibacterial Applications. *J. Mater. Sci. Mater. Med.*, **2011**, 22 (8), 1863–1872. DOI:10.1007/s10856-011-4369-5.
34. Sarvamangala, D. D.; Kondala, K.; Geetha, S.; Manga, and S. (PDF) NANOPARTICLE COATED BANDAGE CLOTH-ANTIMICROBIAL ACTIVITY. *Eur. J. Biomed. Pharm. Sci.*, **2017**, 4 (11).
35. Tripathy, A.; Raichur, A. M.; Chandrasekaran, N.; Prathna, T. C.; Mukherjee, A. Process Variables in Biomimetic Synthesis of Silver Nanoparticles by Aqueous Extract of *Azadirachta Indica* (Neem) Leaves. *J. Nanoparticle Res.*, **2010**, 12 (1), 237–246. DOI:10.1007/s11051-009-9602-5.
36. Hossain, M. A.; Al-Toubi, W. A. S.; Weli, A. M.; Al-Riyami, Q. A.; Al-Sabahi, J. N. Identification and Characterization of Chemical Compounds in Different Crude Extracts from Leaves of Omani Neem. *J. Taibah Univ. Sci.*, **2013**, 7 (4), 181–188. DOI:10.1016/j.jtusci.2013.05.003.
37. Nagar, N.; Devra, V. Green Synthesis and Characterization of Copper Nanoparticles Using *Azadirachta Indica* Leaves. *Mater. Chem. Phys.*, **2018**, 213, 44–51. DOI:10.1016/j.matchemphys.2018.04.007.
38. Dey, A.; Manna, S.; Chattopadhyay, S.; Mondal, D.; Chattopadhyay, D.; Raj, A.; Das, S.; Bag, B. G.; Roy, S. *Azadirachta Indica* Leaves Mediated Green Synthesized Copper Oxide Nanoparticles Induce Apoptosis through Activation of TNF- α and Caspases Signaling Pathway against Cancer Cells. *J. Saudi Chem. Soc.*, **2019**, 23 (2),

222–238. DOI:10.1016/j.jscs.2018.06.011.

39. Subapriya, R.; Nagini, S. Medicinal Properties of Neem Leaves: A Review. *Curr. Med. Chem. Agents*, **2005**, *5* (2), 149–156. DOI:10.2174/1568011053174828.
40. Gollapudi, V. R.; Mallavarapu, U.; Seetha, J.; Akepogu, P.; Amara, V. R.; Natarajan, H.; Anumakonda, V. In Situ Generation of Silver and Silver Oxide Nanoparticles on Cotton Fabrics Using *Tinospora Cordifolia* as Bio Reductant. *SN Appl. Sci.*, **2020**, *2* (3), 1–10. DOI:10.1007/s42452-020-2331-1.
41. Gollapudi, V. R.; Mallavarapu, U.; Seetha, J.; Duddela, V.; Amara, V. R.; Vatti, C. S.; Anumakonda, V. In Situ Generation of Antibacterial Bimetallic Silver and Copper Nanocomposites Using *Tinospora Cordifolia* Leaf Extract as Bio Reductant. *Biointerface Res. Appl. Chem.*, **2020**, *10* (3), 5569–5574. DOI:10.33263/BRIAC103.569574.

Declarations

Funding

Not applicable

Conflicts of interest

None

Availability of data and material

The raw/processed data required to reproduce these findings cannot be shared at this time as the data also forms part of an ongoing study.

Code availability

Not applicable

Authors' contributions

Basa Ashok: Collected primary data, contributed in draft, contributed to the analysis of data, checked the draft, and overall manuscript prepared and finalized the contents.

M.P. Indira Devi: Contributed in writing

P. Sivaranjana: Contributed in writing

AnumakondaVarada Rajulu: Planned and executed the work and contributed in analysis of the results and writing

Faruq Mohammad: Contributed in writing

Sikiru Oluwarotimi Ismail: Contributed in writing

Hamad A. Al-Lohedan: Contributed in writing

Rajini Nagarajan: Supervised and contributed in writing

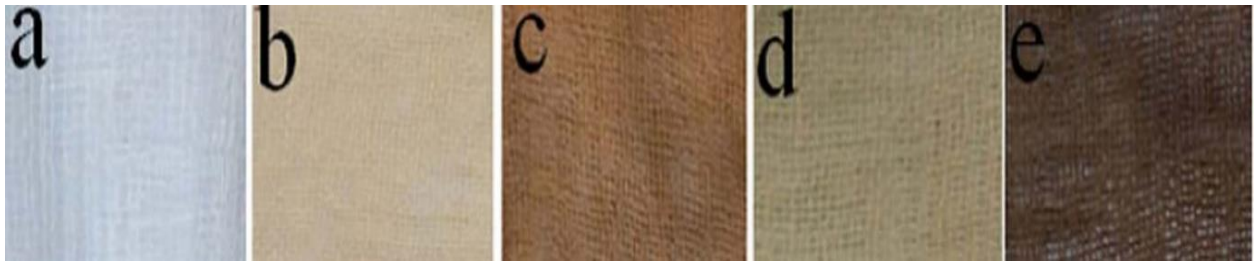


Fig. 1 Photographs of (a) gauge cloth; (b) matrix and NCGCs with (c) AgNPs; (d) CuNPs and (e) BMNPs.

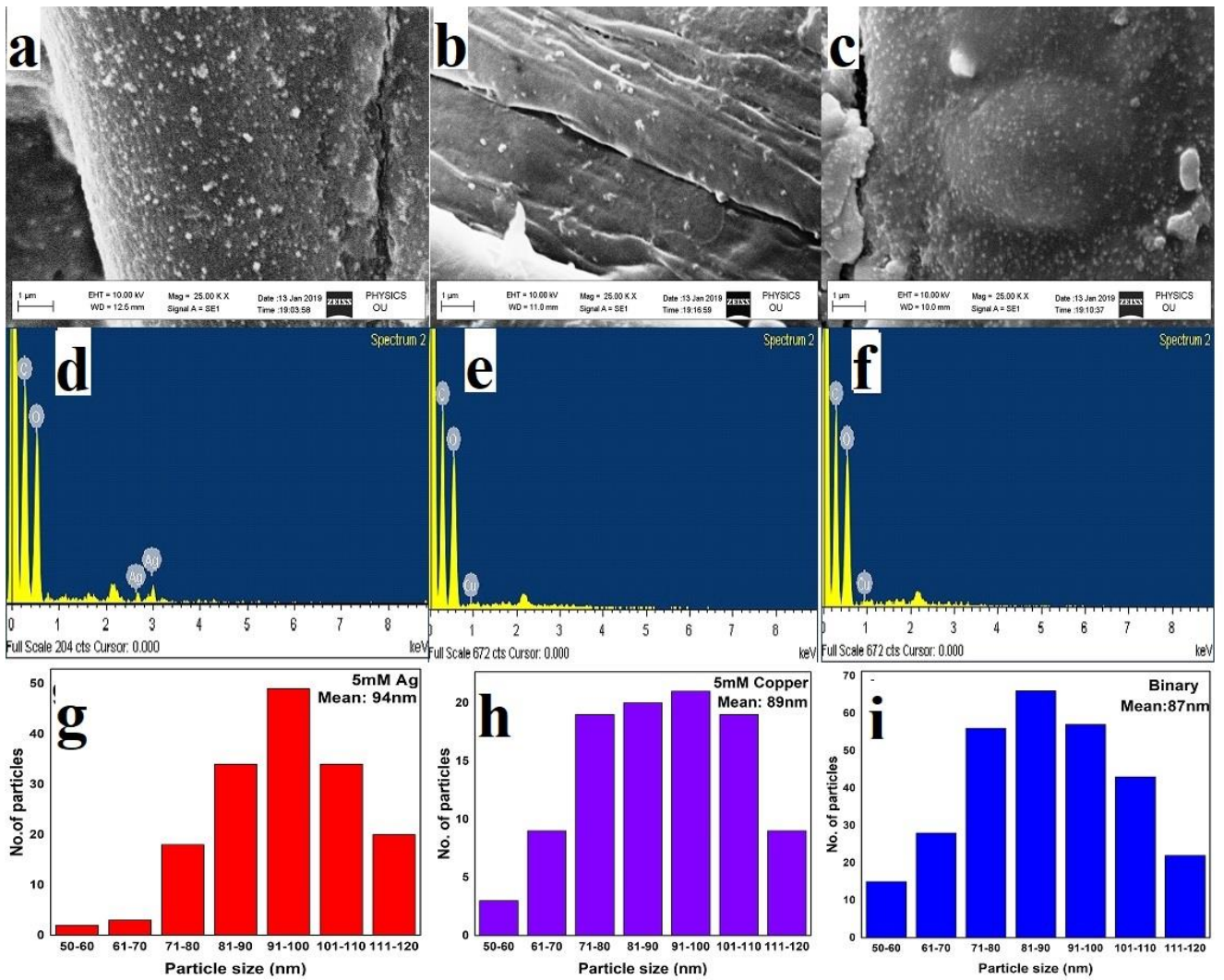


Fig. 2 Images of NCGCs having (a) AgNPs, (b) CuNPs and (c) BMNPs; EDX spectra of NCGCs with (d) AgNPs, (e) CuNPs and (f) BMNPs; Histograms of NCGCs with (g) AgNPs, (h) CuNPs and (i) BMNPs

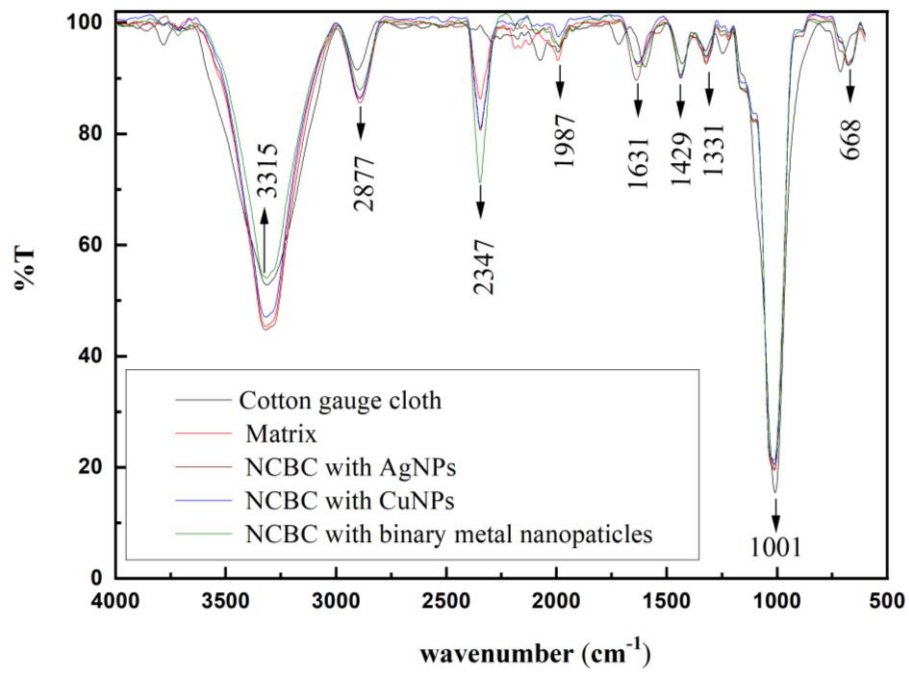


Fig. 3 Spectra (FTIR) of cotton gauge cloth, matrix and NCBCs

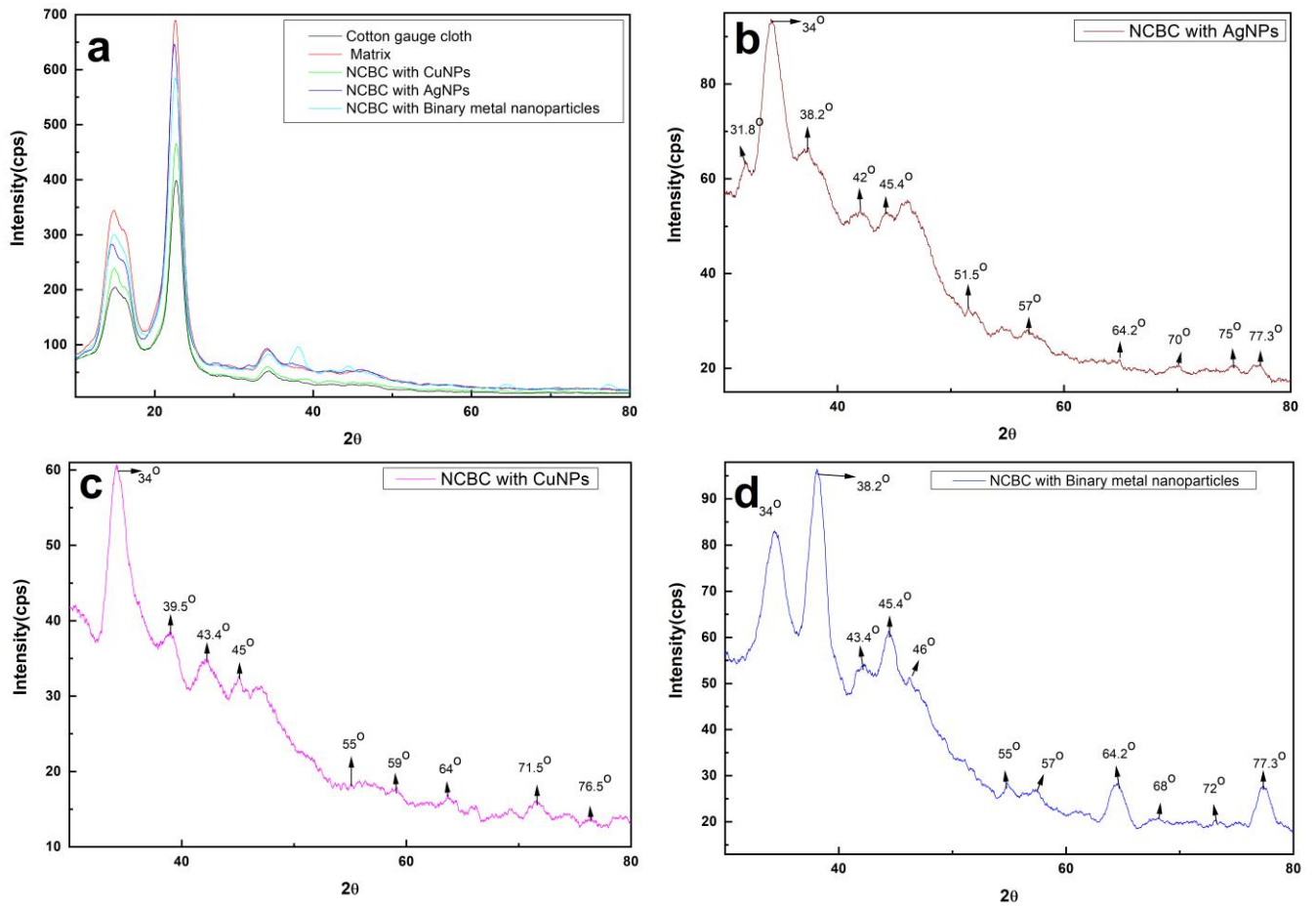
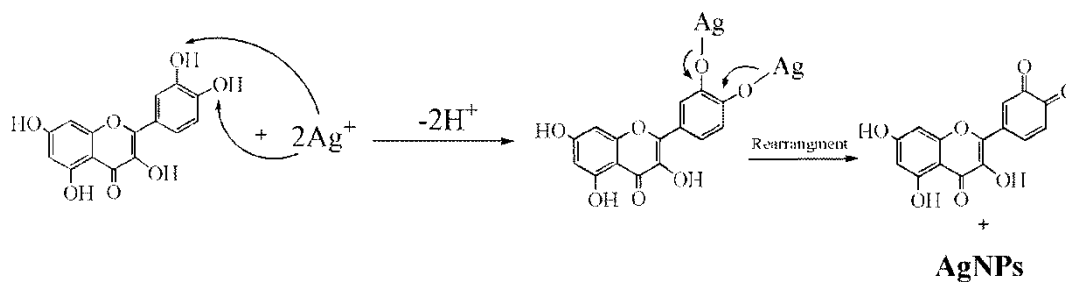
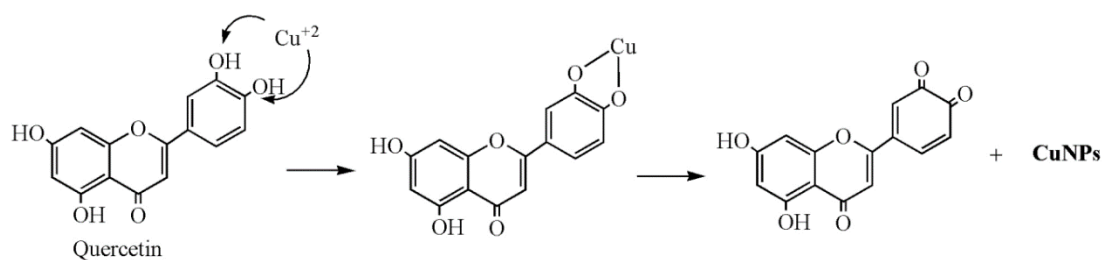


Fig.4 X-ray diffractograms of (a) cotton gauge cloth, matrix and NCBCs; (b) NCBC with in situ generated AgNPs; (c) NCBC with in situ generated CuNPs and (d) NCBC with in situ generated BMNPs.

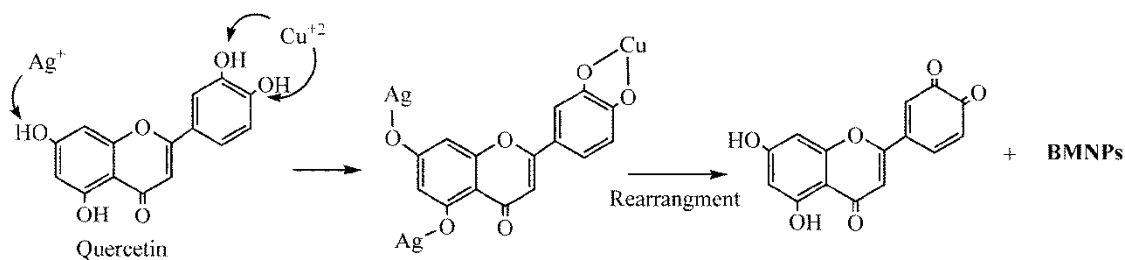
Formation of AgNPs:



Formation of CuNPs:



Formation of Binary metal nanoparticles (BMNPs):



Scheme 1. Mechanism of generation of AgNPs, CuNPs and BMNPs in the NCGCs by the *Azadirachta indica* leaf extract.

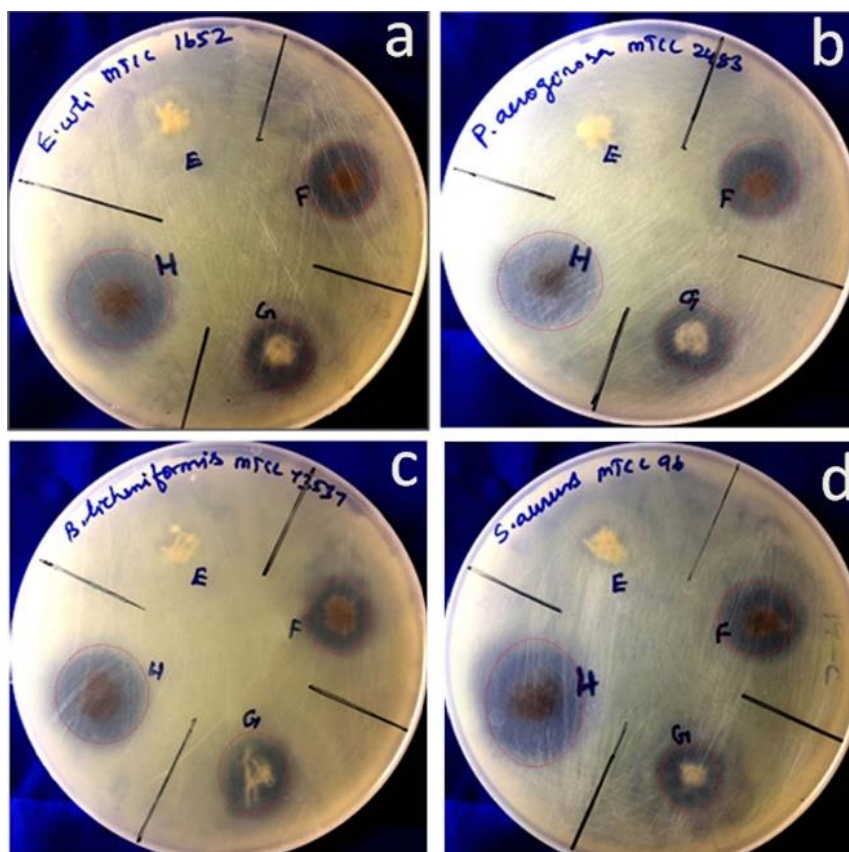


Fig. 5 Images of the inhibition zones formed by Matrix (a) and NCGCs with generated ANPs (b), CuNPs (c) and BMNPs (d) against Nanoparticles against Gram^{-ve} (*E. coli*, *P. aeruginosa*) and Gram^{+ve} (*B. licheniformis*, *S. aureus*) bacteria.

Table 1. Inhibition zone diameters of the matrix and the NCGCs against Gram^{-ve} (*E. coli* and *P. aeruginosa*) and Gram^{+ve} (*B. licheniformis* and *S. aureus*) bacteria.

Sample	Diameter of the Zone of Inhibition (mm)			
	(<i>E. coli</i>)	(<i>P. aeruginosa</i>)	(<i>B. licheniformis</i>)	(<i>S. aureus</i>)
Matrix (E)	0	0	0	0
NCBC with AgNPs (F)	13.3	14.5	11.5	13.6
NCBC with CuNPs (G)	13.7	15.0	14.0	12.9
NCBC with BMNPs (H)	19.5	19.2	17.8	20.1